

*Heteropolyacid anchored on SBA-15
functionalized with 2-aminoethyl
dihydrogen phosphate: a novel and
highly efficient catalyst for one-pot, three-
component synthesis of trisubstituted 1,3-
thiazoles*

Roya Jahanshahi & Batool Akhlaghinia

Research on Chemical Intermediates

ISSN 0922-6168

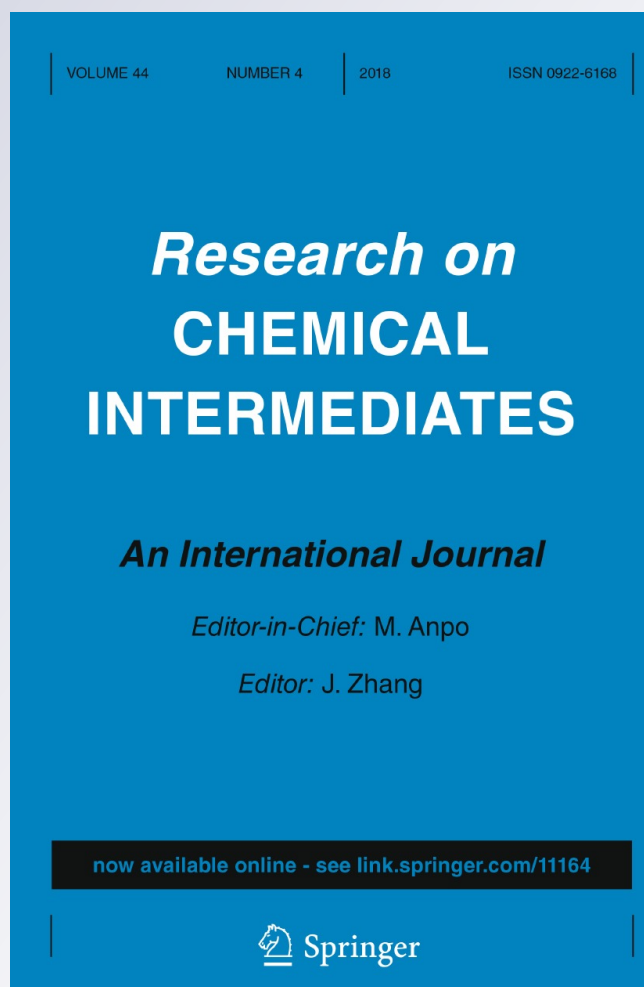
Volume 44

Number 4

Res Chem Intermed (2018)

44:2451-2474

DOI 10.1007/s11164-017-3240-9



Your article is protected by copyright and all rights are held exclusively by Springer Science+Business Media B.V., part of Springer Nature. This e-offprint is for personal use only and shall not be self-archived in electronic repositories. If you wish to self-archive your article, please use the accepted manuscript version for posting on your own website. You may further deposit the accepted manuscript version in any repository, provided it is only made publicly available 12 months after official publication or later and provided acknowledgement is given to the original source of publication and a link is inserted to the published article on Springer's website. The link must be accompanied by the following text: "The final publication is available at link.springer.com".

Heteropolyacid anchored on SBA-15 functionalized with 2-aminoethyl dihydrogen phosphate: a novel and highly efficient catalyst for one-pot, three-component synthesis of trisubstituted 1,3-thiazoles

Roya Jahanshahi¹ · Batool Akhlaghinia¹ 

Received: 6 October 2017 / Accepted: 18 December 2017 / Published online: 28 December 2017
© Springer Science+Business Media B.V., part of Springer Nature 2017

Abstract Heteropolyacid anchored on SBA-15 functionalized with 2-aminoethyl dihydrogen phosphate (SBA-15@AEPH₂-HPA) was synthesized as a novel and highly efficient heterogeneous mesoporous catalyst. Characterization of the as-synthesized catalyst was successfully performed using various techniques such as FT-IR, BET, small-angle XRD, SEM, EDX, TEM, TGA, ICP-OES and elemental analysis. The new catalyst revealed a superb catalytic activity towards the one-pot synthesis of a wide variety of trisubstituted 1,3-thiazole derivatives. This protocol involved the three-component reactions of arylglyoxals, cyclic 1,3-dicarbonyls and thioamides under mild reaction conditions. Surprisingly, the current methodology is far superior to the only literature precedent used in this regard. The most promising features which highlight the presented approach are: furnishing a very important class of pharmaceutically and biologically active 1,3-thiazoles in excellent yields within short reaction times, mildness of the reaction conditions, using water as the reaction media and facile catalyst reusability for at least nine successive runs without any appreciable loss of its activity. Importantly, the small-angle XRD analysis and TEM images of the 9th recovered catalyst clearly proved the privileged durability and stability of the introduced catalytic system, under the applied reaction condition.

Keywords SBA-15@AEPH₂-HPA · Trisubstituted 1,3-thiazoles · Heterogeneous mesoporous catalyst · Heteropolyacid · One-pot reaction

✉ Batool Akhlaghinia
akhlaghinia@um.ac.ir

¹ Department of Chemistry, Faculty of Science, Ferdowsi University of Mashhad, Mashhad 9177948974, Iran

Introduction

Nowadays, novel approaches focus on the development of more environmentally sustainable chemical processes by devising purposive heterogeneous catalytic systems. In this regard, porous materials with high surface areas and very diverse contents have attracted a great deal of attention [1–4]. Among the various types of these porous materials, SBA-15 silicates with unique attributes [5–11], including the high hydrothermal stability, large surface area, regular channels with uniform and tunable pore size and inherent stability in association with admissible flexibility for many surface modifications, are considered as promising candidates for numerous catalytic applications [5–11]. SBA-15 mesoporous materials also have fundamental performances in drug delivery processes, environmental remediation, energy storage, proton conductivity, photoluminescence developments, immobilization of enzymes and, most importantly, manufacturing the heterogeneous catalysts [8–13]. The effectual task-specific design of mesoporous silica-based heterogeneous catalytic systems has been fulfilled by the functionalization of the mesoporous structure with acidic/basic agents containing organic linkers or metal-supported species [14, 15]. The resultant fabricated organic–inorganic hybrid mesoporous materials would be capable of providing a convenient mass transfer throughout organic reaction processes. In other words, they not only afford the effective approach of reactants to the active catalytic sites but also drive away the resulting products into the bulk solution of the reaction to facilitate the reusability of the catalysts [16–20].

Keggin-type heteropolyacids (HPAs), in particular $H_3PW_{12}O_{40}$, have gathered a great deal of attention as promising eco-benign catalysts in many organic transformations and also in Fine Chemistry [21–24]. When compared to mineral acids, HPAs usually exhibit significant turnover numbers and selectivities, besides fewer corrosion problems along with the prevention of side reactions in catalytic processes [25]. Nevertheless, the homogeneous feature of the HPAs, which are plagued with poor stability, low reactivity, and rapid deactivation, has limited their applications [26].

Thiazoles are an imperative class of heterocyclic scaffolds with a ubiquitous range of functions in pharmaceuticals [27–29], natural products [30–33], biologically active alkaloids [34] and materials science (for the preparation of liquid crystals [35, 36], cosmetics [37, 38], etc.). These privileged structural motifs also have prominent biological activities [39–43], such as anti-inflammatory, antibiotic, antibacterial, antitubercular, antitumor, anticonvulsant, antifungal, antiviral, neuroprotective and antioxidant, as well as peptide mimetics [44, 45] and enzyme inhibitors [46, 47]. Furthermore, thiazolium ring is naturally found in the vitamin B₁ (thiamin) structure [48].

The most widely used methodologies for the preparation of substituted thiazoles involves either functionalization of pre-existing thiazole skeletons [49–52] or ring assembly from acyclic substrates [40, 53–59]. Synthesis of thiazoles was first reported in 1887 [60] via the Hantzsch method wherein α -haloketones react with thiourea compounds. Although the Hantzsch-based thiazole synthesis methods are accompanied by excellent yields for simple thiazoles, low thiazole yields were

obtained for some substituted ones. This is due to haloketone dehalogenation during the reaction progress [61, 62].

Considering the above facts, many efforts have been devoted to devising more flexible procedures, particularly for the construction of 1,3-thiazole compounds. In this regard, a number of approaches involving various reagents [63, 64], using multi-step [65] or multicomponent [66–68] reactions, have also been established. Although each of these methods has their own merits, most of them suffer from one or more of the following drawbacks: strict reaction conditions, multistep routes, low availability of the starting materials, tedious workup procedures, low yields of the products, prolonged reaction times and the necessity of applying inert atmospheric conditions. Very recently, Karamthulla and co-workers have reported the microwave-assisted catalyst-free synthesis of trisubstituted 1,3-thiazoles. This approach was conducted via the three-component reactions of arylglyoxals, cyclic 1,3-dicarbonyls, and thioamides at 130 °C in aqueous media [69]. To the best of our knowledge, this is the only reported one-pot three-component reaction in this regard involving such starting materials to deliver the corresponding trisubstituted 1,3-thiazoles.

Bearing in mind the extensive applications of this class of compounds, as well as the novelty of the synthetic procedure, the presentation of a milder, faster and more eco-benign method associated with higher yields of the desired products is much needed. So, in line with the green chemistry legislation, and following our interest in designing new efficient and environmentally benign heterogeneous catalytic systems for organic transformations [70–86], herein, we are reporting a more sustainable, simple and green methodology for the synthesis of trisubstituted 1,3-thiazole derivatives. For this purpose, one-pot three-component reactions were performed between various arylglyoxals, cyclic 1,3-dicarbonyls and thioamides in the presence of catalytic amounts of SBA-15@AEPH₂-HPA as a novel and highly efficient heterogeneous mesoporous catalyst, in mild aqueous media (see Scheme 2).

Experimental

Materials and instruments

All chemical reagents and solvents were purchased from Merck and Sigma-Aldrich and were used as received without any further purification. Mesoporous silica (SBA-15) was prepared by the previously reported method [87].

The purity determinations of the products and the progress of the reactions were accomplished by TLC on silica gel polygram STL G/UV 254 plates. The melting points of the products were determined with an Electrothermal Type 9100 melting point apparatus. Fourier transform infrared (FT-IR) spectra were recorded on pressed KBr pellets using an AVATAR 370 FT-IR spectrometer (Thermo Nicolet, USA) at room temperature in the range between 4000 and 400 cm⁻¹ with a resolution of 4 cm⁻¹. The NMR spectra were recorded on an NMR Bruker Avance spectrometer at 300 MHz in DMSO-*d*₆ and CDCl₃ in the presence of tetramethylsilane as the internal standard, with the coupling constants (*J* values) given in Hz. Elemental analysis was performed using a Thermo Finnigan Flash EA 1112 Series

instrument (furnace: 900 °C; oven: 65 °C; flow carrier: 140 mL min⁻¹; flow reference: 100 mL min⁻¹). Mass spectra were recorded with a CH7A Varianmat Bremem instrument at 70-eV electron impact ionization, in *m/z* (rel%). Brunauer, Emmett and Teller (BET) surface area and pore size distribution were measured on a Belsorp mini II system at -196 °C using N₂ as the adsorbate. Thermogravimetric analysis (TGA) was carried out using a Shimadzu Thermogravimetric Analyzer (TG-50) in the temperature range of 25–900 °C at a heating rate of 10 °C min⁻¹, under air atmosphere. Transmission electron microscopy (TEM) was performed with a Leo 912 AB microscope (Zeiss, Germany) with an accelerating voltage of 120 kV. Scanning electron microscopy (SEM) images were also recorded using a Leo1450 VP scanning electron microscope equipped with an SC7620 energy-dispersive X-ray spectrometer (EDX) presenting a 133-eV resolution at 20 kV. The crystalline structure of the catalyst was analyzed by small-angle X-ray diffraction (small-angle XRD) using a PANalytical Company X'Pert PRO MPD diffractometer operated at 40 kV and 40 mA, utilizing Cu K α radiation ($\lambda = 0.154$ nm), (at a step size of 0.020° and step time of 2 s.). All yields refer to the isolated products after purification by recrystallization.

Preparation of mesoporous silica (SBA-15) (I)

An amount of 4.0 g of pluronic P123 triblock copolymer surfactant was dissolved as a template in a solution containing double-distilled H₂O (30 mL) and 2 M HCl (80.5 mL). Then, TEOS (tetraethyl orthosilicate) (40.8 mmol, 8.5 g) was added to the resulting mixture and continuous stirring was conducted at 40 °C for 8 h. The resultant solution was next transferred into a Teflon-lined stainless steel autoclave and kept at 100 °C for 20 h without stirring. After cooling to room temperature, the afforded material was filtered and washed with distilled H₂O, before being dried overnight at 65 °C. Ultimately, the as-synthesized product was calcined at 550 °C for 6 h to eliminate the copolymer template.

Preparation of SBA-15 functionalized with 2-aminoethyl dihydrogen phosphate (SBA-15@AEPH₂) (II)

The synthesized SBA-15 (1 g) was dispersed in deionized water (20 mL) for 20 min. Then, AEPH₂ (0.7 g, 5 mmol) was added portion by portion to the resulting suspension, and the obtained mixture was vigorously stirred at room temperature for 12 h. Subsequently, the resulting SBA-15@AEPH₂ was collected by centrifugation, washed with ethanol (3 × 15 mL) and dried at ambient temperature, overnight.

Preparation of heteropolyacid anchored on SBA-15 functionalized with 2-aminoethyl dihydrogen phosphate (SBA-15@AEPH₂-HPA) (III)

A solution of HPA (2.88 g, 1 mmol) in 5 mL methanol was added dropwise to a suspension of SBA-15@AEPH₂ (1.0 g) in methanol (50 mL). Afterwards, the resulting

mixture was stirred at 50 °C for 12 h. Finally, the final designed catalyst was centrifuged, washed repeatedly with ethanol and air-dried.

Typical procedure for the synthesis of 3-(2,4-diphenylthiazol-5-yl)-4-hydroxy-2H-chromen-2-one (4a)

SBA-15@AEPH₂-HPA (0.02 g, 0.13 mol%) was added to a solution of 4-hydroxycoumarin (1 mmol, 0.162 g), phenylglyoxal (1 mmol, 0.134 g) and thiobenzamide (1 mmol, 0.137 g) in H₂O (3 mL). The resulting mixture was magnetically stirred at 50 °C for 15 min. The reaction progress was monitored by TLC (*n*-hexane:EtOAc, 1:1). Upon completion of the reaction, hot ethanol was added to the reaction mixture and the heterogeneous catalyst was separated by centrifugation. Next, the separated catalyst was washed with ethanol (3 × 15 mL) to be ready for utilizing in the next run. Then, the filtrate was evaporated and the resulting crude product was recrystallized from ethanol to afford the pure **4a** product (0.39 g, 98%).

Spectral data

3-(2,4-Diphenylthiazol-5-yl)-4-hydroxy-2H-chromen-2-one (4a) (Yield: 98%); white solid; mp 163–164 °C (from EtOH) (Lit [69]. 162–164 °C); ¹H NMR: δH (300 MHz; DMSO-*d*₆; Me₄Si) 11.89 (1 H, br s, OH), 8.04 (2 H, br d, *J* = 6.7 Hz, Ar-H), 7.94 (1 H, d, *J* = 6.9 Hz, Ar-H), 7.74 (2 H, d, *J* = 7.2 Hz, Ar-H), 7.68 (1 H, d, *J* = 7.2 Hz, Ar-H), 7.54–7.59 (3 H, m, Ar-H), 7.44 (1 H, d, *J* = 8.1 Hz, Ar-H), 7.30–7.40 (4 H, m, Ar-H); ¹³C NMR: δC (75 MHz; DMSO-*d*₆; Me₄Si) 166.85, 164.53, 161.61, 154.13, 153.28, 135.34, 133.56, 130.81, 129.76, 128.82, 128.39, 127.85, 126.51, 124.61, 124.56, 123.17, 116.92, 116.50, 96.20; MS, *m/z* 397 (M⁺, 99%), 291 (37), 276 (47, M - C₇H₅O₂³⁻), 192 (25, M - C₁₀H₅O₃S³⁻), 121 (99, M - C₁₇H₁₀NOS³⁻), 77 (92, M - C₁₈H₁₀NO₃S³⁻).

3-(2-(4-Chlorophenyl)-4-phenylthiazol-5-yl)-4-hydroxy-2H chromen-2-one (4b) (Yield: 96%); pale yellow solid; mp 256–258 °C (from EtOH) (Lit [69]. 257–259 °C); FT-IR (KBr): ν_{max}/cm⁻¹ 3064, 3027, 1666, 1609, 1563, 1517, 1485, 1398, 1343, 1232, 1184, 1153, 1098, 985; ¹H NMR: δH (300 MHz; DMSO-*d*₆; Me₄Si) 8.07 (2 H, d, *J* = 8.1 Hz, Ar-H), 7.96 (1 H, d, *J* = 7.8 Hz, Ar-H), 7.71–7.75 (3 H, m, Ar-H), 7.63 (2 H, d, *J* = 8.1 Hz, Ar-H), 7.47 (2 H, d, *J* = 8.4 Hz, Ar-H), 7.32–7.43 (3 H, m, Ar-H); ¹³C NMR: δC (75 MHz; DMSO-*d*₆; Me₄Si) 165.65, 164.23, 161.53, 154.43, 153.26, 135.46, 135.14, 133.76, 132.35, 129.88, 128.91, 128.57, 128.24, 127.87, 124.76, 124.54, 123.40, 117.00, 116.24, 96.39; MS, *m/z* 432 (M⁺, 98%), 434 (44, M + 2), 290 (46), 154 (98, M - C₁₇H₁₂NO₃), 120 (97), 77 (43, M - C₁₈H₉ClNO₃S³⁻).

4-Hydroxy-3-(2-(4-methoxyphenyl)-4-phenylthiazol-5-yl)-2H-chromen-2-one (4c) (Yield: 98%); white solid; mp 171–172 °C (from EtOH) (Lit [69]. 173–175 °C); MS, *m/z* 427 (M⁺, 99%), 428 (98, M + 1), 409 (96), 291 (43), 150 (80, M - C₁₇H₁₃NO₃), 134 (83, M - C₁₇H₉O₃S²⁻), 121 (63, M - C₁₈H₁₂NO₂S³⁻).

3-(2-(4-Chlorophenyl)-4-(4-methoxyphenyl)thiazol-5-yl)-4-hydroxy-2H-chromen-2-one (4d) (Yield: 95%); pale yellow solid; mp 222–223 °C (from EtOH) (Lit [69]. 223–225 °C), $^1\text{H NMR}$: δH (300 MHz; DMSO- d_6 ; Me $_4$ Si) 8.06 (2 H, d, $J = 3.9$ Hz, Ar–H), 7.96 (1 H, d, $J = 3.9$ Hz, Ar–H), 7.71–7.76 (1 H, m, Ar–H), 7.65 (2 H, br t, $J = 9.9$ Hz, Ar–H), 7.39–7.49 (4 H, m, Ar–H), 6.94 (2 H, d, $J = 8.1$ Hz, Ar–H), 3.75 (3 H, s, OCH $_3$); $^{13}\text{C NMR}$: δC (75 MHz; DMSO- d_6 ; Me $_4$ Si) 165.35, 164.31, 161.56, 159.54, 154.19, 153.28, 135.34, 133.72, 132.43, 129.88, 129.18, 128.20, 127.71, 124.75, 124.55, 116.99, 116.35, 114.32, 55.55; MS, m/z 462 (M^+ , 99%), 464 (28, $\text{M} + 2$), 320 (23), 120 (91), 92 (11, $\text{M} - \text{C}_{19}\text{H}_{12}\text{ClNO}_3\text{S}^2$).

3-(2,4-Bis(4-methoxyphenyl)thiazol-5-yl)-4-hydroxy-2H-chromen-2-one (4e) (Yield: 96%); pale yellow solid; 248–249 °C (from EtOH) (Lit [69]. 249–251 °C); MS, m/z 457 (M^+ , 85%), 458 (78, $\text{M} + 1$), 455 ($\text{M} - 2$), 304 (79, $\text{M} - \text{C}_8\text{H}_{11}\text{OS}$), 289 (68), 174 (37), 120 (78, $\text{M} - \text{C}_{18}\text{H}_{13}\text{NO}_4\text{S}$).

3-Hydroxy-2-(4-(4-methoxyphenyl)-2-phenylthiazol-5-yl)-5,5-dimethylcyclohex-2-en-1-one (4f) (Yield: 96%); pale yellow solid; mp 220–221 °C (from EtOH) (Lit [69]. 219–221 °C); MS, m/z 405 (M^+ , 29%), 407 (28, $\text{M} + 2$), 289 (95), 137 (91, $\text{M} - \text{C}_{16}\text{H}_{14}\text{NOS}$), 121 (47, $\text{M} - \text{C}_{17}\text{H}_{20}\text{NO}_3$), 104 (78), 77 (96, $\text{M} - \text{C}_{18}\text{H}_{18}\text{NO}_3\text{S}$).

2-(2,4-Bis(4-methoxyphenyl)thiazol-5-yl)-3-hydroxy-5,5-dimethylcyclohex-2-en-1-one (4g) (Yield: 98%); white solid; mp, 292–293 °C (from EtOH); FT-IR (KBr): $\nu_{\text{max}}/\text{cm}^{-1}$ 3068, 2994, 2960, 2888, 2834, 1605, 1577, 1518, 1494, 1468, 1362, 1310, 1244, 1175, 1108, 1029, 980; $^1\text{H NMR}$: δH (300 MHz; DMSO- d_6 ; Me $_4$ Si) 11.29 (1 H, br s, OH), 7.89 (2 H, d, $J = 8.4$ Hz, Ar–H), 7.61 (2 H, d, $J = 8.4$ Hz, Ar–H), 7.83 (2 H, d, $J = 8.4$ Hz, Ar–H), 6.93 (2 H, d, $J = 8.4$ Hz, Ar–H), 3.85 (3 H, s, OCH $_3$), 3.79 (3 H, s, OCH $_3$), 2.40 (4 H, s, 2CH $_2$), 1.08 (6 H, s, 2CH $_3$); δC (75 MHz; DMSO- d_6 ; Me $_4$ Si) 165.22, 161.10, 159.08, 152.18, 129.14, 128.71, 127.83, 126.73, 122.79, 115.02, 113.91, 106.35, 55.82, 55.55, 31.97, 28.48; MS, m/z 564 (M^+ , 84%), 566 (70, $\text{M} + 2$), 519 (13, $\text{M} - \text{NO}_2^+$), 473 (41, $\text{M} - 2\text{NO}_2$), 442 (100, $\text{M} - \text{C}_6\text{H}_4\text{NO}_2$), 269 (83), 45 (12, $\text{M} - \text{C}_{32}\text{H}_{29}\text{N}_3\text{O}_4$); Elemental analysis: Found: C, 68.94; H, 5.79; N, 3.22%. Calc. for $\text{C}_{25}\text{H}_{25}\text{NO}_4\text{S}$: C, 68.90; H, 5.77; N, 3.19%.

2-(2,4-Diphenylthiazol-5-yl)-3-hydroxy-5,5-dimethylcyclohex-2-en-1-one (4h) (Yield: 98%); white solid; mp 202–203 °C (from EtOH) (Lit [69]. 204–206 °C); $^1\text{H NMR}$: δH (300 MHz; DMSO- d_6 ; Me $_4$ Si) 11.39 (1 H, br s, OH), 8.07 (1 H, br d, $J = 8.7$ Hz, Ar–H), 7.74 (2 H, br d, $J = 7.5$ Hz, Ar–H), 7.63 (1 H, br d, $J = 8.7$ Hz, Ar–H), 7.47 (2 H, br d, $J = 9.0$ Hz, Ar–H), 7.32–7.43 (4 H, m, Ar–H), 2.40 (4 H, s, 2CH $_2$), 1.08 (6 H, s, 2CH $_3$); δC (75 MHz; DMSO- d_6 ; Me $_4$ Si) 165.56, 152.77, 135.97, 133.78, 130.48, 129.70, 128.57, 128.37, 128.01, 127.92, 127.74, 126.34, 125.53, 106.13, 31.99, 28.46; MS, m/z 375 (M^+ , 60%), 373 (100, $\text{M} - 2\text{H}$), 322 (46), 289 (20, $\text{M} - \text{C}_5\text{H}_{10}\text{O}^3$), 270 (47, $\text{M} - \text{C}_7\text{H}_7\text{N}$), 121 (28), 104 (84, $\text{M} - \text{C}_{16}\text{H}_{15}\text{O}_2\text{S}^2$).

2-(2-(4-Chlorophenyl)-4-phenylthiazol-5-yl)-3-hydroxy-5,5-dimethylcyclohex-2-en-1-one (4i) (Yield: 96%); white solid; mp 206–207 °C (from EtOH) (Lit [69]. 206–208 °C); FT-IR (KBr): $\nu_{\max}/\text{cm}^{-1}$ 3060, 2951, 2921, 2867, 1586, 1511, 1484, 1443, 1372, 1304, 1249, 1142, 1090, 1013, 976; ^1H NMR: δH (300 MHz; DMSO- d_6 ; Me $_4$ Si) 11.41 (1 H, br s, OH), 7.99 (1 H, d, $J = 8.7$ Hz, Ar-H), 7.68 (1 H, d, $J = 6.9$ Hz, Ar-H), 7.59 (2 H, d, $J = 8.4$ Hz, Ar-H), 7.30–7.41 (5 H, m, Ar-H), 2.40 (4 H, s, 2CH $_2$), 1.08 (6 H, s, 2CH $_3$); δC (75 MHz; DMSO- d_6 ; Me $_4$ Si) 164.19, 152.95, 135.83, 134.99, 132.60, 129.76, 128.58, 128.09, 128.01, 127.92, 126.02, 106.02, 31.98, 28.45; MS, m/z 409 (M $^+$, 99%), 411 (33, M + 2), 294 (41), 269 (66, M - C $_8$ H $_{12}$ O $_2$), 323 (43, M - C $_5$ H $_{10}$ O $^{3-}$), 138 (29, M - C $_{15}$ H $_{10}$ CIN S^+).

2-(2-(4-Bromophenyl)-4-phenylthiazol-5-yl)-3-hydroxy-5,5-dimethylcyclohex-2-en-1-one (4j) (Yield: 97%); white solid; mp 226–227 °C (from EtOH); FT-IR (KBr): $\nu_{\max}/\text{cm}^{-1}$ 3056, 3019, 2955, 2929, 2868, 1571, 1483, 1361, 1323, 1260, 1147, 1069, 1029, 977; ^1H NMR: δH (300 MHz; DMSO- d_6 ; Me $_4$ Si) 11.42 (1 H, br s, OH), 7.92 (2 H, d, $J = 8.1$ Hz, Ar-H), 7.73 (2 H, d, $J = 8.4$ Hz, Ar-H), 7.68 (2 H, d, $J = 6.9$ Hz, Ar-H), 7.30–7.42 (3 H, m, Ar-H), 2.40 (4 H, s, 2CH $_2$), 1.08 (6 H, s, 2CH $_3$); δC (75 MHz; DMSO- d_6 ; Me $_4$ Si) 164.27, 152.97, 135.82, 132.93, 132.67, 128.59, 128.22, 128.10, 127.92, 126.07, 123.73, 106.00, 31.98, 28.46; Elemental analysis: Found: C, 60.80; H, 4.44; N, 3.08%. Calc. for C $_{23}$ H $_{20}$ BrNO $_2$ S: C, 60.77; H, 4.42; N, 3.05%.

3-Hydroxy-2-(2-(4-methoxyphenyl)-4-phenylthiazol-5-yl)-5,5-dimethylcyclohex-2-en-1-one (4k) (Yield: 98%); white solid; 150–151 °C (from EtOH) (Lit [69]. 149–151 °C); MS, m/z 405 (M $^+$, 100%), 406 (78, M + 1), 153 (64, M - C $_{16}$ H $_{19}$ NO $_2$), 134 (88), 105 (35, M - C $_{17}$ H $_{18}$ NO $_2$ S $^+$).

3-(2,4-Diphenylthiazol-5-yl)-4-hydroxy-1-methylquinolin-2(1H)-one (4l) (Yield: 97%); white solid; mp 196–198 °C (from EtOH) (Lit [69]. 197–199 °C); ^1H NMR: δH (300 MHz; DMSO- d_6 ; Me $_4$ Si) 10.92 (1 H, br s, OH), 8.00–8.06 (3 H, m, Ar-H), 7.71–7.73 (3 H, m, Ar-H), 7.56–7.59 (4 H, m, Ar-H), 7.25–7.36 (4 H, m, Ar-H), 3.35 (3 H, s, NCH $_3$); δC (75 MHz; DMSO- d_6 ; Me $_4$ Si) 166.51, 161.92, 159.71, 153.60, 140.02, 135.57, 133.73, 132.47, 130.71, 129.80, 128.74, 128.22, 127.81, 126.46, 124.80, 124.38, 122.18, 115.99, 115.28, 102.31, 29.90; MS, m/z 410 (M $^+$, 96%), 412 (64, M + 2), 391 (55), 305 (92, M - C $_7$ H $_7$ N 2), 105 (41, M - C $_{18}$ H $_{11}$ NO $_2$ S 2).

3-(2-(4-Chlorophenyl)-4-phenylthiazol-5-yl)-4-hydroxy-1-methylquinolin-2(1H)-one (4m) (Yield: 95%); pale yellow solid; mp 118–119 °C (from EtOH) (Lit [69]. 117–119 °C); FT-IR (KBr): $\nu_{\max}/\text{cm}^{-1}$ 3051, 2929, 2880, 1691, 1624, 1563, 1501, 1487, 1417, 1328, 1205, 1161, 1091, 1042, 984; MS, m/z 445 (M $^+$, 100%), 447 (54, M + 2), 358 (39), 303 (99), 174 (23, M - C $_{15}$ H $_9$ CIN S^+), 137 (23, M - C $_{17}$ H $_6$ CINOS 2).

4-Hydroxy-3-(2-(4-methoxyphenyl)-4-phenylthiazol-5-yl)-1-methylquinolin-2(1H)-one (4n) (Yield: 98%); white solid; mp 271–273 °C (from EtOH) (Lit [69]. 272–274 °C); MS, m/z 440 (M^+ , 98%), 441 (68, $M + 1$), 305 (90, $M - C_8H_9NO^2$), 274 (25, $M - C_8H_8NOS^2$), 243 (22), 133 (49, $M - C_{18}H_{13}NO_2S^2$).

4-Hydroxy-3-(4-(4-methoxyphenyl)-2-phenylthiazol-5-yl)-1-methylquinolin-2(1H)-one (4o) (Yield: 95%); white solid; mp 269–270 °C (from EtOH) (Lit [69]. 270–272 °C); MS, m/z 440 (M^+ , 100%), 442 (86, $M + 2$), 333 (94, $M - C_7H_7O$), 318 (72), 305 (28, $M - C_7H_5NS^2$), 290 (21).

3-(2-(4-Chlorophenyl)-4-(4-methoxyphenyl)thiazol-5-yl)-4-hydroxy-1-methylquinolin-2(1H)-one (4p) (Yield: 93%); pale yellow solid; mp 257–258 °C (from EtOH) (Lit [69]. 256–258 °C); 1H NMR: δH (300 MHz; DMSO- d_6 ; Me $_4$ Si) 10.87 (1 H, br s, OH), 8.05 (1 H, d, $J = 8.7$ Hz, Ar-H), 8.01 (1 H, br d, $J = 8.4$ Hz, Ar-H), 7.72 (1 H, br t, $J = 8.4$ Hz, Ar-H), 7.57–7.65 (6 H, m, Ar-H), 7.31 (1 H, t, $J = 7.5$ Hz, Ar-H), 6.89 (2 H, d, $J = 8.7$ Hz, Ar-H), 3.73 (3 H, s, OCH $_3$); 3.65 (3 H, s, NCH $_3$); δC (75 MHz; DMSO- d_6 ; Me $_4$ Si) 164.87, 161.94, 159.36, 153.55, 140.04, 135.13, 132.62, 132.46, 129.85, 129.11, 128.09, 128.02, 124.41, 122.17, 116.04, 115.26, 114.16, 102.24, 55.52, 29.89; MS, m/z 475 (M^+ , 98%), 476 (82, $M + 1$), 369 (23, $M - C_7H_7N^2$), 334 (55), 319 (23, $M - C_7H_6ClS$), 105 (28, $M - C_{19}H_{12}ClNO_3S^2$).

2-(2-(4-Chlorophenyl)-4-phenylthiazol-5-yl)-3-hydroxy-1H-inden-1-one (4q) (Yield: 97%); pale red solid; mp 77–78 °C (from EtOH) (Lit [69]. 77–79 °C); 1H NMR: δH (300 MHz; DMSO- d_6 ; Me $_4$ Si) 7.99 (2 H, d, $J = 8.1$ Hz, Ar-H), 7.77 (3 H, d, $J = 7.5$ Hz, Ar-H), 7.47–7.60 (3 H, m, Ar-H), 7.28–7.41 (5 H, m, Ar-H); δC (75 MHz; DMSO- d_6 ; Me $_4$ Si) 188.24, 162.89, 151.20, 137.59, 136.57, 134.74, 132.75, 131.73, 129.69, 128.77, 128.37, 128.15, 127.92, 127.76, 127.55, 125.03, 120.03, 101.05; MS, m/z 419 (19, $M + 2$), 417 (M^+ , 73%), 415 (73, $M - 2$), 219 (58), 138 (75, $M - C_{17}H_{10}O_2S^2$), 105 (100), 77 (73, $M - C_{18}H_9ClNO_2S$).

2-(2,4-Diphenylthiazol-5-yl)-3-hydroxy-1H-inden-1-one (4r) (Yield: 92%); red solid; mp 75–76 °C (from EtOH) (Lit [69]. 76–78 °C); FT-IR (KBr): ν_{max}/cm^{-1} 3061, 2923, 2851, 1710, 1665, 1595, 1560, 1492, 1413, 1397, 1251, 1091, 1013, 988; MS, m/z 381 (M^+ , 60%), 380 (97, $M - 1$), 223 (45), 137 (96, $M - C_{17}H_8O_2$), 105 (96), 77 (97, $M - C_{18}H_{10}NO_2S$).

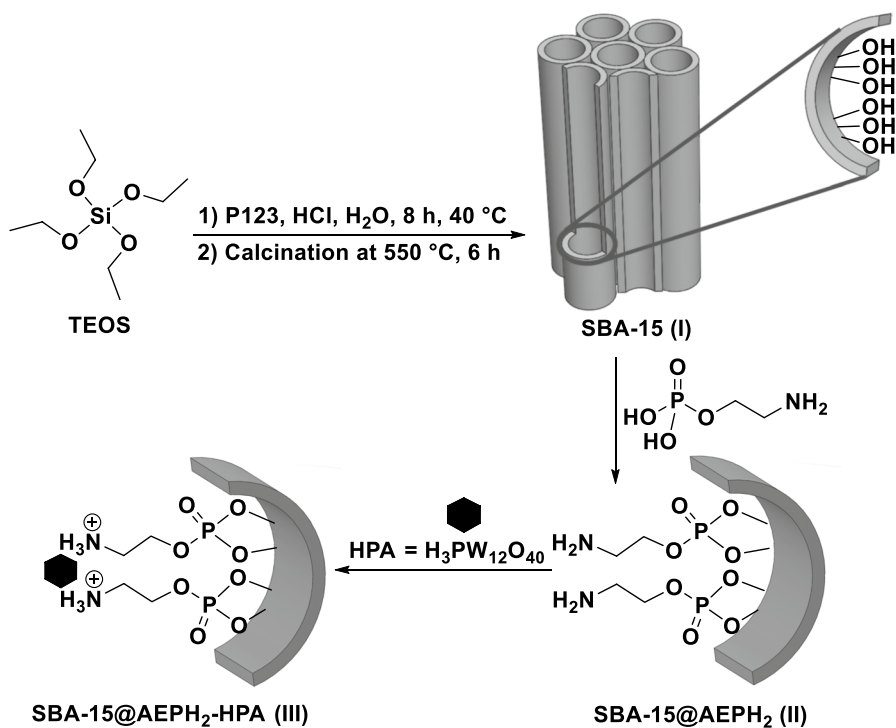
3-Hydroxy-2-(2-(4-methoxyphenyl)-4-phenylthiazol-5-yl)-1H-inden-1-one (4s) (Yield: 98%); red solid; mp 83–84 °C (from EtOH) (Lit [69]. 82–84 °C); MS, m/z 411 (M^+ , 70%), 410 (84, $M - 1$), 238 (54), 151 (87, $M - C_{17}H_{12}NO_2$), 134 (99), 104 (83, $M - C_{18}H_{13}NO_2S^3$).

Results and discussion

SBA-15@AEPH₂-HPA as a new heterogeneous mesoporous catalyst was synthesized according to the pathway displayed in Scheme 1. The structure and morphology of the introduced catalyst was investigated and fully characterized by a series of techniques comprising FT-IR, BET surface area analysis, small-angle XRD, SEM, EDX, TEM, TGA, inductively coupled plasma optical emission spectroscopy (ICP-OES) and elemental analysis (CHNS). The resulting data from these techniques corroborated the successful preparation of the newly synthesized mesoporous catalyst.

Characterization of SBA-15@AEPH₂-HPA

FT-IR spectroscopy was conducted for every step of the mesocatalyst synthesis to verify the successful functionalization of the SBA-15 surface (Fig. 1). As presented in Fig. 1a, the absorption bands attributed to the bending, symmetric and asymmetric stretching vibrations of Si–O–Si were observed at 465, 803 and 1085 cm⁻¹, respectively [70]. Two characteristic bands at 1633 and 3426 cm⁻¹ are in turn ascribed to the bending and stretching vibration modes of the surface-attached hydroxyl groups (Si–OH) and the adsorbed water molecules [88].



Scheme 1 An overview of the synthesis of SBA-15@AEPH₂-HPA

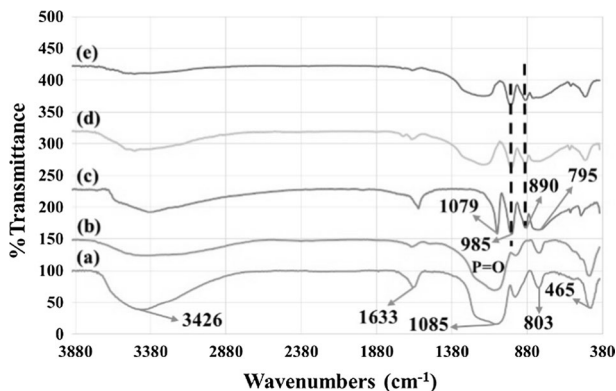


Fig. 1 FT-IR spectra of **a** SBA-15, **b** SBA-15@AEPH₂, **c** H₃PW₁₂O₄₀, **d** fresh SBA-15@AEPH₂-HPA, and **e** 9th recovered SBA-15@AEPH₂-HPA

In the FT-IR spectrum of SBA-15@AEPH₂ (Fig. 1b), the appearance of the broad absorption band in the region of about 3600–3000 cm⁻¹ could be assigned to the overlapping of uncoated O–H and NH₂ stretching modes [89]. Furthermore, the distinctive bands observed at 2960 and 2882 cm⁻¹ could be allocated to the asymmetric and symmetric methylene C–H stretching vibrational frequencies, respectively [90]. Also, the stretching vibration of P = O bond, which was visualized at 1150 cm⁻¹ [89], would clearly confirm the successful chemical attachment of AEPH₂ onto the mesoporous silica surface. As illustrated in the FT-IR spectrum of H₃PW₁₂O₄₀ (Fig. 1c), the characteristic vibrational frequencies related to the Keggin units appeared at 1079, 985, 890 and 795 cm⁻¹. These absorption bands are assigned, respectively, to the stretching vibrations of tetrahedral P–O bonds, terminal W=O bonds and two types of bridging W–O–W bonds of the Keggin clusters [91].

After anchoring the heteropolyacid on the SBA-15@AEPH₂, the above-mentioned diagnostic vibrational peaks could be still found in the FT-IR spectrum; however, a slight diminution in peak intensities was perceived [92] (Fig. 1d). In any case, the vibrations of tetrahedral P–O bonds of Keggin units may interfere with the characteristic asymmetric stretching modes of Si–O bonds in the SBA-15 structure (at 1085 cm⁻¹) [92, 93]. The above results not only imply the strong interaction of the Keggin units and support material but also assert that the primary Keggin structure remains intact after the immobilization process.

Figure 2 shows the N₂ adsorption–desorption isotherms and the corresponding BJH pore-size distribution curves of the SBA-15 and SBA-15@AEPH₂-HPA. As is apparent in Fig. 2a, c, a typical type IV isotherm with a H1 hysteresis loop was evident for both pristine SBA-15 and SBA-15@AEPH₂-HPA, which is the characteristic of mesoporous materials with uniform cylindrical pores [94]. Table 1 demonstrates the corresponding average surface area, pore volume and mean pore diameter of both SBA-15 and SBA-15@AEPH₂-HPA. The BET surface area, pore volume and pore diameter of the intact SBA-15 were 737, 1.2 and 6.6, respectively, which dropped to some extent after the modification process. These results confirm

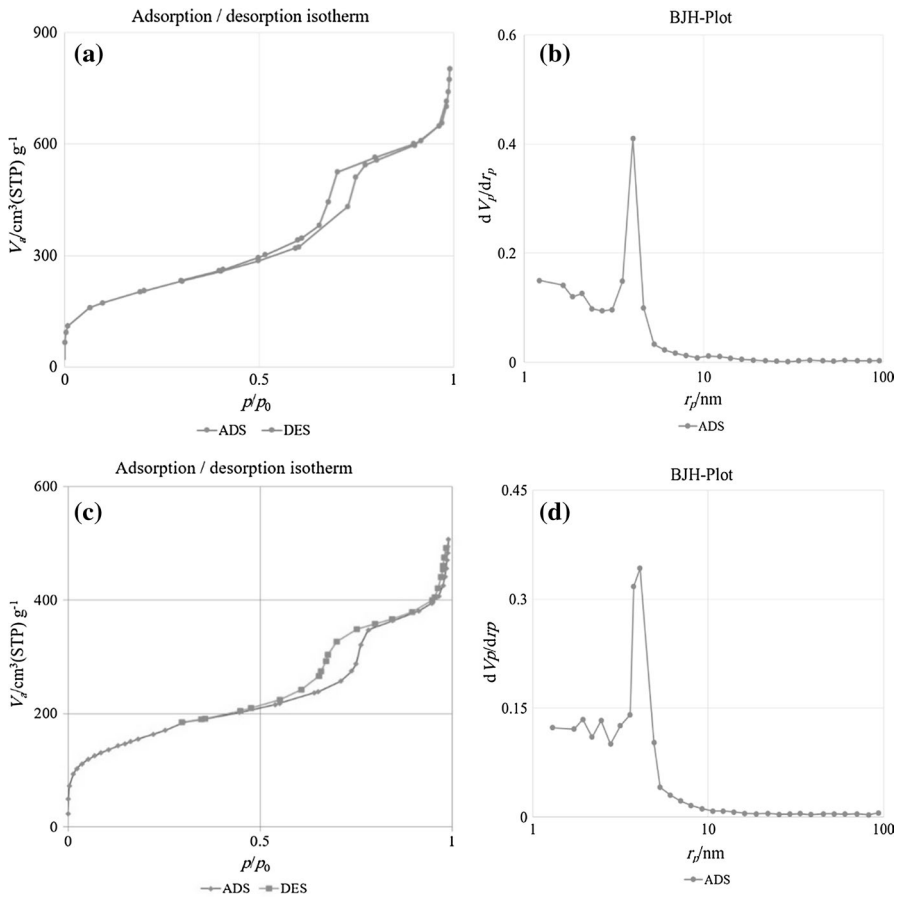


Fig. 2 Nitrogen adsorption–desorption isotherms (a, c) and pore size distribution isotherms (b, d) of SBA-15 and SBA-15@AEPH₂-HPA

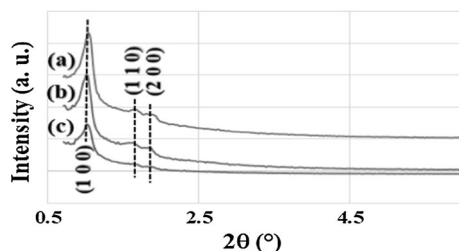
Table 1 Specific surface area (S_{BET}), pore volume and mean pore diameter of SBA-15 and SBA-15@AEPH₂-HPA

Sample	S_{BET} ($m^2 g^{-1}$)	Pore volume ($cm^3 g^{-1}$)	Mean pore diameter (nm)
SBA-15	737	1.2	6.6
SBA-15@AEPH ₂ -HPA	561	0.8	5.9

the efficacious functionalization of the SBA-15 framework. Moreover, the BJH calculations revealed a uniform pore-size distribution accompanied by a high-intensity peak, which ascertains the high regularity of the mesostructure (Fig. 2b, d).

Small-angle XRD was implemented to gain further insight into the structural properties of the novel synthesized catalyst (Fig. 3). As is obvious, the presence

Fig. 3 Small-angle XRD patterns of **a** SBA-15, **b** fresh SBA-15@AEPH₂-HPA and **c** 9th recovered SBA-15@AEPH₂-HPA



of characteristic peaks appeared below 2° attributed to the (100), (110) and (200) reflection planes are also readily recognized from the XRD patterns of SBA-15, SBA-15@AEPH₂-HPA and 9th recovered SBA-15@AEPH₂-HPA. These indicative diffraction peaks clearly offered a two-dimensional hexagonal structure [95–100] for the pristine SBA-15, final designed catalyst and the recovered catalyst after 9 runs.

SEM analysis was additionally conducted to investigate the morphology of the newly designed catalyst (Fig. 4a, b). Obviously, a very satisfying uniform rod-like morphology can be inferred from the SEM images of the SBA-15@AEPH₂-HPA catalyst.

Furthermore, the EDX analysis indicates the presence of Si, O, C, P, N and W elements (Fig. 5).

This analysis established that H₃PW₁₂O₄₀ heteropolyacid is successfully immobilized onto the SBA-15@AEPH₂ surface.

TEM images of SBA-15@AEPH₂-HPA were recorded and are presented in Fig. 6. It can be easily deduced from these images that the as-synthesized catalyst has an ordered hexagonally mesoporous structure with an average pore size of about 5.9 nm, along with a supreme regularity in the channel framework (Fig. 6a).

The attained TEM results were in a very good agreement with the small-angle XRD, as well as with data obtained from nitrogen adsorption–desorption analyses. Consequently, it can readily be seen that the regularity of the mesoscopic channels was well retained after the modification process, which further endorses the durability and stability of the as-synthesized catalyst upon the functionalization procedure.

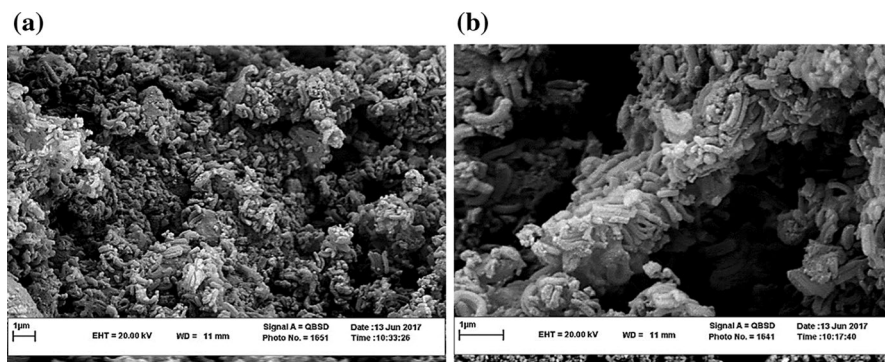


Fig. 4 SEM images of SBA-15@AEPH₂-HPA (**a**, **b**)

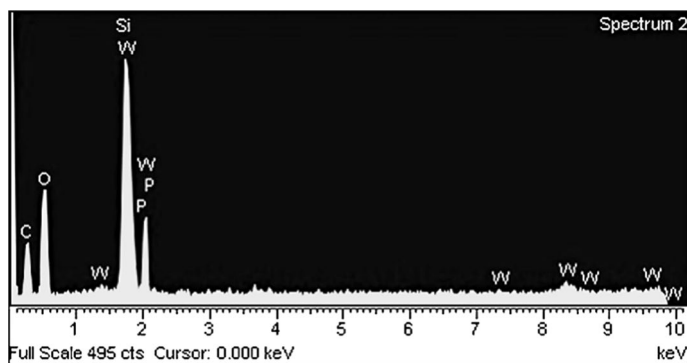


Fig. 5 EDX analysis of SBA-15@AEPH₂-HPA

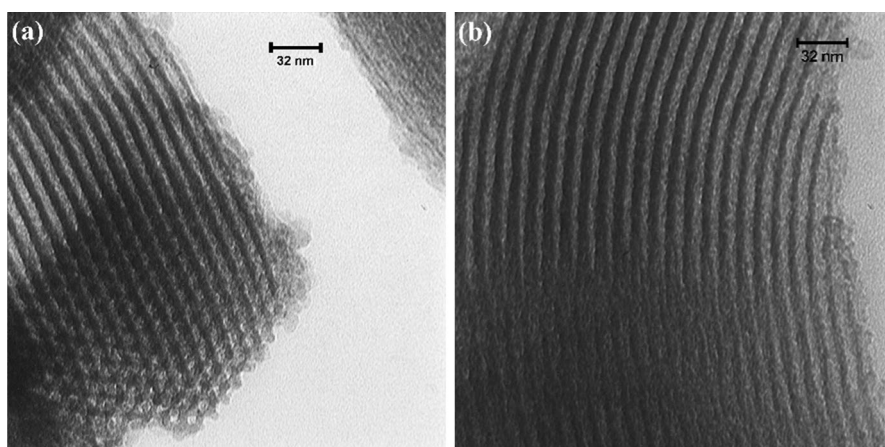
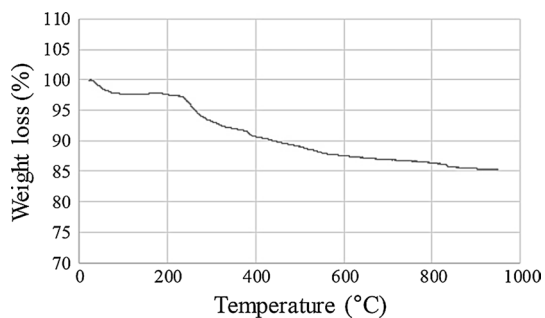


Fig. 6 TEM images of **a** fresh SBA-15@AEPH₂-HPA and **b** 9th recovered SBA-15@AEPH₂-HPA

Fig. 7 TGA thermogram of SBA-15@AEPH₂-HPA



TGA was carried out to determine the thermal stability and organic content of the novel synthesized mesocatalyst (Fig. 7). The obtained results revealed two significant weight losses at different temperature ranges. The first weight loss of about 2%

below 200 °C could be assigned to the removal of the trapped physically adsorbed water molecules. The second significant weight loss, which began at about 200 °C and continued up to 850 °C, can be attributed to the elimination of the organic functional groups along with the heteropolyacid organic segments incorporated into the SBA-15 mesostructure (12.5%). These observations evidently documented the excellent practical thermal stability of the fabricated mesocatalyst even at elevated temperatures (200 °C). According to the TGA data, the amount of organic motif supported on the SBA-15 framework was estimated to be 0.73 mmol g⁻¹. These findings were in a very good agreement with the obtained elemental analysis data (N = 1.03% and C = 2.08%).

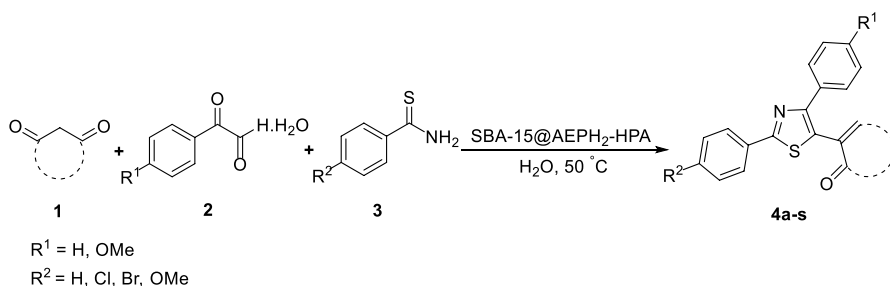
Moreover, ICP-OES analysis of the fresh SBA-15@AEPH₂-HPA confirmed the existence of 0.26 mmol of tungsten element, which was fastened on 1.00 g of the mesocatalyst, as a result of the support decoration by heteropolyacid.

Catalytic synthesis of trisubstituted 1,3-thiazoles

Following the successful preparation and full characterization of SBA-15@AEPH₂-HPA, to explore the potential activity of such a new heterogeneous mesocatalyst, its catalytic applicability was evaluated for the green synthesis of trisubstituted 1,3-thiazoles. For this purpose, one-pot three-component reactions between various arylglyoxals, cyclic 1,3-dicarbonyls and thioamides were conducted under the mild aqueous media (Scheme 2).

In the preliminary assessment, the reaction conditions were optimized by varying the solvent, temperature and catalyst amount towards the model reaction of 4-hydroxycoumarin (1 mmol), phenylglyoxal monohydrate (1 mmol) and thiobenzamide (1 mmol) (Table 2).

As observed, a blank experiment in the absence of a catalyst in solvent-free condition, either at room temperature or 100 °C, was accompanied by none of the desired product, even after a prolonged reaction time (Table 2, entries 1 and 2). Also, the reaction was promoted to some extent in the presence of 0.13 mol% (0.02 g) of SBA-15@AEPH₂-HPA, under the ambient temperature (Table 2, entry 3).



Scheme 2 Synthesis of trisubstituted 1,3-thiazoles in the presence of SBA-15@AEPH₂-HPA, under mild aqueous media

Table 2 One-pot, three-component synthesis of 3-(2,4-diphenylthiazol-5-yl)-4-hydroxy-2H-chromen-2-one (**4a**) under different reaction conditions

Entry	Catalyst (mol%)	Solvent	Temp. (°C)	Time (min)	Isolated yield (%)
1	–	–	r.t.	24 h	0
2	–	–	100	24 h	0
3	0.13	–	r.t.	1 h	25
4	0.13	H ₂ O	r.t.	1 h	55
5	0.13	EtOH	r.t.	2 h	45
6	0.13	EtOH/H ₂ O (1:1)	r.t.	1.5 h	50
7	0.13	CH ₃ CN	r.t.	2 h	40
8	0.13	Toluene	r.t.	2 h	25
9	0.13 ^a	H ₂ O	50	15	98
10	0.13	H ₂ O	100	15	98
11	0.10	H ₂ O	50	20	79
12	0.15	H ₂ O	50	15	98
13	0.13 ^b	H ₂ O	50	1 h	Trace
14	0.13 ^c	H ₂ O	50	1 h	Trace
15	0.13 ^d	H ₂ O	50	1 h	20

Reaction conditions: 4-hydroxycoumarin (1 mmol), phenylglyoxal monohydrate (1 mmol) and thiobenzamide (1 mmol)

^a0.13 mol% of the catalyst is equals to 0.02 g of the catalyst

^bReaction was performed in the presence of SBA-15 as catalyst

^cReaction was performed in the presence of SBA-15@AEPH₂ as catalyst

^dReaction was performed in the presence of H₃PW₁₂O₄₀ as catalyst

By keeping other conditions the same, to survey the influence of solvent on the reaction progress the model reaction was conducted in a number of solvents including H₂O, EtOH, H₂O/EtOH [1/1 (v/v)], CH₃CN and toluene (Table 2, entries 4–8). These experiments found that H₂O was superior to all of the tested solvents with regards to the concepts of green chemistry. To our great delight, significant improvement in the product yield was achieved when the reaction temperature was increased to 50 °C (Table 2, entry 9). More elevated temperatures (100 °C) did not have any positive effect on the reaction progress (Table 2, entry 10). In continuation of our efforts to seek more optimal conditions, the effect of catalyst amount was next evaluated. As demonstrated in Table 2, by diminishing the catalyst amount to 0.10 mol%, the product yield was significantly decreased (Table 2, entry 11). On the other hand, upon increasing the amount of SBA-15@AEPH₂-HPA, no further improvement was observed in the reaction rate (Table 2, entry 12). Consequently, the reaction was strongly affected by the amount of the mesocatalyst. In the next step, to show the crucial effect of SBA-15@AEPH₂-HPA on the reaction progress, the catalytic performances of SBA-15 and SBA-15@AEPH₂ were also checked under the same reaction conditions (Table 2, entries 13 and 14). In this regard, the product yields were trace amounts, even after a long reaction time. In addition, by

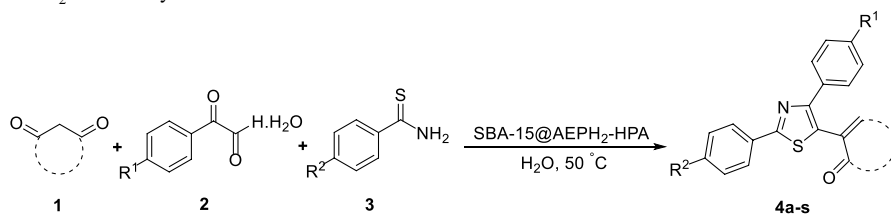
keeping the other conditions the same, the effect of utilizing HPA as a catalyst was also investigated. Nevertheless, the result was far from satisfactory in this context (Table 2, entry 15). Despite that HPA is a homogenous strong acid in nature and is expected to have more activity, the catalytic activity of SBA-15@AEPH₂-HPA was a great deal higher in such a transformation. The reason may come from the fact that the mesoporous SBA-15@AEPH₂-HPA catalyst acts as a smart nanoreactor, which could increase the impressive collisions of the reactants within the catalyst structure, leading to the straightforward formation of high-yielding products. However, in the presence of the homogeneous HPA, the reaction might be associated with the formation of undesired by-products. These findings clearly highlighted the essential role of SBA-15@AEPH₂-HPA in the catalytic development of such a transformation.

Having the optimized reaction conditions in hand, we next investigated the generality of the novel synthesized catalytic system towards the preparation of diverse trisubstituted 1,3-thiazole derivatives. For this purpose, the reactions of various structurally divergent cyclic 1,3-dicarbonyls, arylglyoxals and thiobenzamides were evaluated under the optimized reaction conditions, and the results are summarized in Table 3.

It is worth mentioning that the scope of the synthesis of these valuable class of compounds has become more widespread with the capability of applying different cyclic 1,3-dicarbonyls such as 4-hydroxycoumarin, dimedone, 4-hydroxy-1-methyl-2(1*H*)-quinolone and indane-1,3-dione. In all of these cases, well-yielded desired products were delivered within short reaction times. Gratifyingly, thiobenzamide derivatives bearing either electron-withdrawing or electron-releasing groups and also phenyl/4-methoxyphenyl glyoxal derivatives operated with almost equal efficiency to furnish the corresponding thiazoles in good to excellent yields. These observations further confirmed the privileged applicability of SBA-15@AEPH₂-HPA mesoporous catalyst in catalyzing the one-pot, three-component synthesis of a broad range of trisubstituted 1,3-thiazoles.

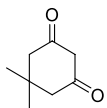
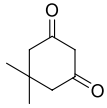
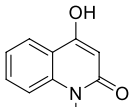
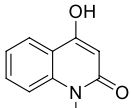
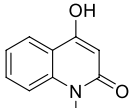
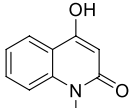
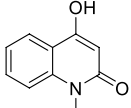
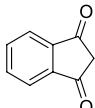
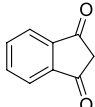
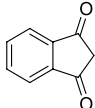
All of the synthesized products were known compounds except compounds **4g** and **4j**, and their structures were approved by comparison of their melting points and mass spectrometry with those of authentic compounds. A number of selected compounds were further characterized by FT-IR, ¹H NMR and ¹³C NMR spectroscopy, which were closely matched with literature data. The obtained elemental analysis data of the novel synthesized compounds (**4g** and **4j**) were also in a very good conformity with the presented structures. It is noteworthy that, in the FT-IR spectra of most of the purified products, the existence of absorption bands at about 3432–3452 (OH), 1571–1710 (C=O), 1577–1665 (C=N), 1511–1595 and 1468–1492 cm⁻¹ (aromatic C=C), obviously confirmed the corresponding product structures.

Moreover, ¹H NMR spectra of most of the products displayed the appearance of a broad singlet resonating at around 11.89–10.87 ppm, which was attributed to the hydroxyl group proton. In addition, in the ¹H NMR spectra of the products, the existence of aromatic rings relating to protons ranging from 8.09 to 6.88 ppm obviously verified the structure of the desired products. In the ¹³C NMR spectra, the products' proposed structures were well certified by the existence of the requisite numbers of distinct resonances. Likewise, the presentation of distinctive signals at 188–164 and 164–152 ppm, which are allocated in turn to the S–C=N and O–C=O bonds, were

Table 3 Substrate scope for the synthesis of trisubstituted 1,3-thiazoles using mesoporous SBA-15@AEPH₂-HPA catalyst

Entry	1,3-Dicarbonyl compound	R ¹	R ²	Product	Time (min)	Isolated yield (%)
1		H	H	4a	15	98
2		H	Cl	4b	20	96
3		H	OMe	4c	15	98
4		OMe	Cl	4d	20	95
5		OMe	OMe	4e	20	96
6		OMe	H	4f	15	96
7		OMe	OMe	4g	15	98
8		H	H	4h	15	98
9		H	Cl	4i	15	96

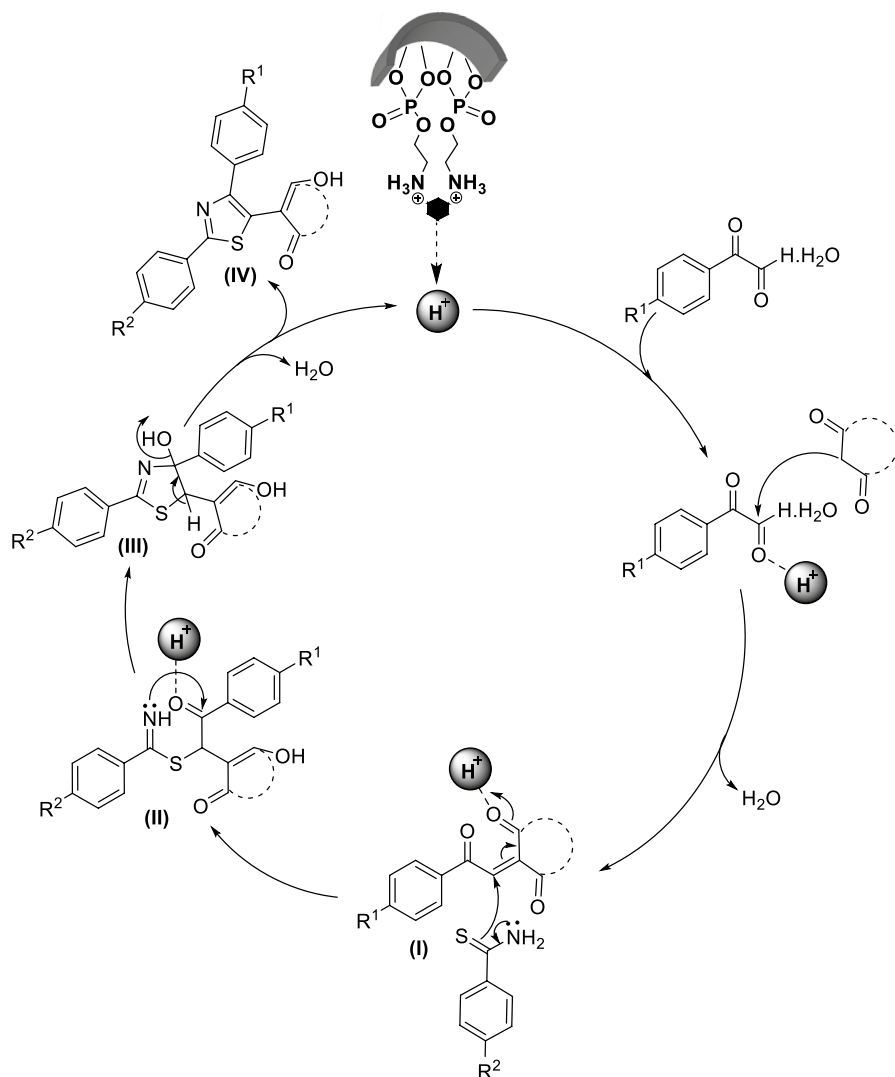
Table 3 (continued)

Entry	1,3-Dicarbonyl compound	R ¹	R ²	Product	Time (min)	Isolated yield (%)
10		H	Br	4j	15	97
11		H	OMe	4k	15	98
12		H	H	4l	10	97
13		H	Cl	4m	15	95
14		H	OMe	4n	10	98
15		OMe	H	4o	15	95
16		OMe	Cl	4p	25	93
17		H	Cl	4q	20	97
18		H	H	4r	20	92
19		H	OMe	4s	15	98

Reaction conditions: cyclic1, 3-dicarbonyls (1 mmol), arylglyoxals (1 mmol), thioamides (1 mmol), SBA-15@AEPH₂-HPA (0.02 g, 0.13 mol%), in H₂O (3 mL) at 50 °C

perceived from the ^{13}C NMR spectra. Further, mass spectra of all prepared products revealed molecular ion peaks at their respective m/e .

By analogy with our investigations, the plausible mechanistic pathway for the synthesis of trisubstituted 1,3-thiazoles in the presence of the SBA-15@AEPH₂-HPA mesocatalyst is proposed in Scheme 3. In the initial step, SBA-15@AEPH₂-HPA activates the aldehyde carbonyl group of the arylglyoxal compound to make it susceptible to nucleophilic attack of the cyclic 1,3-dicarbonyl compound through a Knoevenagel-type condensation reaction. Thereupon, the activated resultant



Scheme 3 A plausible reaction mechanism for the synthesis of trisubstituted 1,3-thiazoles in the presence of SBA-15@AEPH₂-HPA

intermediate **I** undergoes a nucleophilic attack by the thioamide compound via the thia-Michael addition reaction, which subsequently leads to the formation of intermediate **II**. In the next step, the intramolecular nucleophilic attack of nitrogen to the activated carbonyl caused the delivery of intermediate **III** upon cyclization. Eventually, the final desired product (**IV**) was afforded as a result of the loss of H₂O. Then, the regenerated acidic mesocatalyst re-enters the catalytic cycle. Further studies to elucidate the details of the mechanism are ongoing.

Reusability of the mesoporous SBA-15@AEPH₂-HPA catalyst

The recycling and recovery of the heterogeneous catalytic systems are very vital aspects from economical, environmental and industrial viewpoints. Along this line, the reusability of the mesoporous catalyst was next explored for the model reaction under the optimized conditions. At the end of each run, the mesoporous SBA-15@AEPH₂-HPA catalyst was separated by centrifugation, washed with ethanol, and vacuum-dried at 50 °C to be ready for re-employing directly in another fresh reaction mixture. The results clearly indicate that the aforementioned catalytic system was not only very active but also extremely stable and reusable under the chosen reaction conditions. This result arises from the fact that almost no significant deactivation of the mesoporous catalyst occurred during the reaction cycles (Fig. 8). However, the gradual decrease in the activity of the regenerated mesoporous catalyst after 9 sequences might be principally due to the partial saturation of the mesochannels containing catalytic active sites during the reaction process.

To gain a deep insight into the structural stability of SBA-15@AEPH₂-HPA after 9 runs, the recovered catalyst was also characterized via FT-IR, small-angle XRD and TEM analyses.

It is important to note that the FT-IR spectrum of the 9th recovered mesoporous catalyst (Fig. 1e) illustrates the thorough preservation of the characteristic absorption bands in terms of the shape, position and relative intensity. These findings

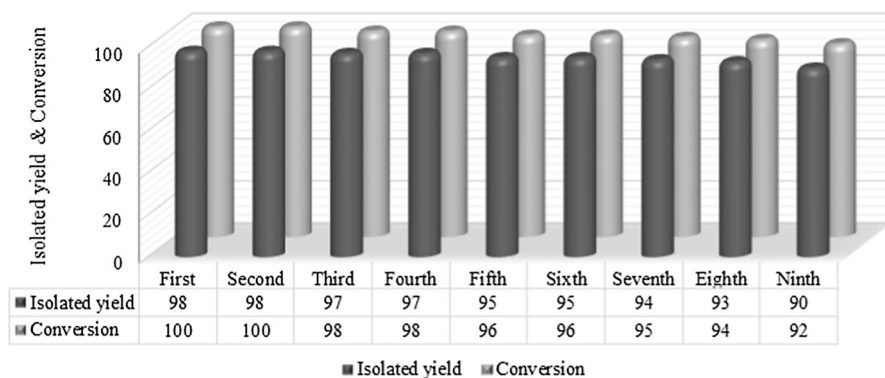


Fig. 8 Recyclability study of mesoporous SBA-15@AEPH₂-HPA catalyst for the model reaction

evidently affirmed that only insignificant changes occurred in the chemical structure of the functional groups and the hydrogen bonding network of the mesoporous catalyst.

Moreover, three well-resolved peaks below 2° indexed as (100), (110) and (200) reflections clearly existed in the small-angle XRD patterns of SBA-15, fresh SBA-15@AEPH₂-HPA and the 9th recovered catalyst. These characteristic peaks indicate the 2-D hexagonal symmetry (P6 mm) of these materials (Fig. 3) [10, 95–100]. However, a total decrement in the intensity of these respective peaks (especially the intensity of the (100) reflection) was recognized after the modification process (Fig. 3b). This attenuation might be caused by the effect of pore-filling of functional groups, which may be able to diminish the scattering contrast between the SBA-15 lattice and the filled pores with organic moieties, which would be accompanied by the fractional loss of the ordered silica structure due to the organic motifs incorporation [10, 101]. More prominently, the small-angle XRD pattern of the 9th recovered SBA-15@AEPH₂-HPA mesocatalyst indicated an inconsiderable broadening or shifting of peaks comparing to the small-angle XRD pattern of the fresh one (Fig. 3c). The durability of the (100), (110) and (200) reflections not only ascertained the structural stability and existence of a long-range ordering of the mesochannels but also the survival of the undisturbed pore wall thickness, even after several courses of the reaction [102].

Satisfyingly, the TEM image of the 9th recycled catalyst demonstrated the conservation of well-ordered arrays of SBA-15@AEPH₂-HPA, even after nine consecutive runs (Fig. 6b).

Based on ICP-OES analysis, although the measured W content of the freshly prepared SBA-15@AEPH₂-HPA was estimated to be 0.26 mmol per 1.00 g of the catalyst, the 9th recovered catalyst consisted of 0.24 mmol of W per 1.00 g of the mesocatalyst. This means that the amount of leached tungsten element from the mesoporous platform is negligible.

Conclusion

In summary, SBA-15@AEPH₂-HPA, as a novel, efficient, heterogeneous mesoporous catalyst, was synthesized and fully characterized by different techniques including FT-IR, BET, small-angle XRD, SEM, EDX, TEM, TGA, ICP-OES and CHNS analyses. The efficiency of the newly fabricated mesoporous catalyst was monitored for the preparation of a wide range of trisubstituted 1,3-thiazole derivatives through the three-component reactions of arylglyoxals, cyclic 1,3-dicarbonyls, and thioamides, under mild conditions. Surprisingly, the current methodology is far superior to the only literature precedent found in this regard, especially in terms of the mildness of the reaction conditions, the reaction operational simplicity, attaining higher-yielded products within shorter reaction times and simple purification of the products (without the use of column chromatography). Also, the developed protocol not only involves the preparation of the imperative pharmaceutically and biologically active 1,3-thiazole derivatives but also associates with the prominent

reusability of the mesocatalyst. In addition, conducting the reaction in aqueous media also supports the present approach towards green chemistry.

Acknowledgements The authors gratefully acknowledge the partial support of this study by Ferdowsi University of Mashhad Research Council (Grant No. p/3/39490).

References

1. M. Pramanik, A. Bhaumik, *J. Mater. Chem. A* **1**, 11210 (2013)
2. J. Karger, R. Valiullin, *Chem. Soc. Rev.* **42**, 4172 (2013)
3. H.Y. Hsueh, C.T. Yao, R.M. Ho, *Chem. Soc. Rev.* **44**, 1974 (2015)
4. J. Li, A. Corma, J. Yu, *Chem. Soc. Rev.* **44**, 7112 (2015)
5. P. Yang, D. Zhao, D.I. Margolese, B.F. Chmelka, G.D. Stucky, *Nature (London, U.K.)* **396**, 152 (1998)
6. S. Rostamnia, N. Nouruzi, H. Xin, R. Luque, *Catal. Sci. Technol.* **5**, 199 (2015)
7. Z. Wu, L. Zhang, Q. Guan, M. Fu, D. Ye, T. Wu, *Mater. Res. Bull.* **70**, 567 (2015)
8. C. Liang, M.C. Wei, H.H. Tseng, E.C. Shu, *Chem. Eng. J.* **223**, 785 (2013)
9. D. Zhao, J. Feng, Q. Huo, N. Melosh, G.H. Fredrickson, B.F. Chmelka, G.D. Stucky, *Science* **279**, 548 (1998)
10. A. Wróblewska, E. Makuch, *J. Adv. Oxid. Technol.* **17**, 44 (2014)
11. B. Karimi, F. Mansouri, M. Khorasani, *Curr. Org. Chem.* **20**, 349 (2016)
12. S. Rostamnia, E. Doustkhah, *RSC Adv.* **4**, 28238 (2014)
13. V. Meynen, P. Cool, E.F. Vansant, *Microporous Mesoporous Mater.* **125**, 170 (2009)
14. A. Taguchi, F. Schüth, *Microporous Mesoporous Mater.* **77**, 1 (2005)
15. M. Nandi, J. Mondal, K. Sarkar, Y. Yamauchi, A. Bhaumik, *Chem. Commun.* **47**, 6677 (2011)
16. H. Lia, M. Yang, Q. Pu, *Microporous Mesoporous Mater.* **148**, 166 (2012)
17. C.M. Crudden, M. Sateesh, R. Lewis, *J. Am. Chem. Soc.* **127**, 10045 (2005)
18. S. Rostamnia, K. Lamei, F. Pourhassan, *RSC Adv.* **4**, 59626 (2014)
19. A. Corma, *Chem. Rev.* **97**, 2373 (1997)
20. A. Corma, H. Garcia, *Adv. Synth. Catal.* **348**, 1391 (2006)
21. I.V. Kozhevnikov, *Catalysts for Fine Chemicals, Catalysis by Polyoxometalates*, vol. 2 (Wiley, Chichester, 2002)
22. Y. Kamiya, T. Okuhara, M. Misono, A. Miyaji, K. Tsuji, T. Nakajo, *Catal. Surv. Asia* **12**, 101 (2008)
23. E.V. Gusevskaya, *ChemCatChem* **6**, 1506 (2014)
24. A.E.R.S. Khder, H.M.A. Hassanc, M.S. El-Shall, *Appl. Catal. A. Gen.* **487**, 110 (2014)
25. R.F. Cotta, K.A. da Silva Rocha, E.F. Kozhevnikova, I.V. Kozhevnikov, E.V. Gusevskaya, *Catal. Today* **289**, 14 (2017)
26. G.D. Yadav, D.P. Tekale, *Catal. Today* **237**, 54 (2014)
27. G. Pattenden, *J. Heterocycl. Chem.* **29**, 607 (1992)
28. S.K. Sharma, M. Tandon, J.W. Lown, *J. Org. Chem.* **65**, 1102 (2000)
29. S.I. El-Desoky, S.B. Bondock, H.A. Etman, A.A. Fadda, M.A. Metwally, *Sulfur Lett.* **26**, 127 (2003)
30. G. Pattenden, S.M. Thom, *J. Chem. Soc. Perkin Trans. 1*, 1629 (1993)
31. A.K. Todorova, F. Juettner, A. Linden, T. Pluess, W.V. Philipsborn, *J. Org. Chem.* **60**, 7891 (1995)
32. D.J. Faulkner, *Nat. Prod. Rep.* **18**, 1 (2001)
33. J.O. Melby, N.J. Nard, D.A. Mitchell, *Curr. Opin. Chem. Biol.* **15**, 369 (2011)
34. Z. Jin, *Nat. Prod. Rep.* **28**, 1143 (2011)
35. K.A. Trumm, H.J. Sattler, S. Postius, I. Szelenyi, W. Schunack, *Arzneim. Forsch.* **35**, 573 (1985)
36. D.J. Kempf, H.L. Sham, K.C. Marsh, C.A. Flentge, D. Betebenner, B.E. Green, E. McDonald, S. Vasavanonda, A. Saldivar, N.E. Wideburg, W.M. Kati, L. Ruiz, C. Zhao, L. Fino, J. Patterson, A. Molla, J.J. Plattner, D.W. Norbeck, *J. Med. Chem.* **41**, 602 (1998)
37. K. Dolling, H. Zschacke, H. Schubert, *J. Prakt. Chem.* **321**, 643 (1979)
38. A. Mori, A. Sekiguchi, K. Masui, T. Shimada, M. Horie, K. Osakada, M. Kawamoto, T. Ikeda, *J. Am. Chem. Soc.* **125**, 1700 (2003)

39. B. Chen, W. Heal, in *Comprehensive Heterocyclic Chemistry III*, vol. 4, ed. by A.R. Atritzky, C.A. Ramsden, E.F.V. Scriven, R.J.K. Taylor (Elsevier, Oxford, 2008), p. 635
40. P. Wipf, *Chem. Rev.* **95**, 2115 (1995)
41. Y.J. Wu, B.V. Yang, Five membered ring systems: with N and S (Se, Te) atoms, in *Progress in Heterocyclic Chemistry*, vol. 18, ed. by G.W. Gribble, J.A. Joule (Elsevier, Oxford, 2007), p. 247
42. Z. Jin, *Nat. Prod. Rep.* **26**, 382 (2009)
43. S.M. Mustafa, V.A. Nair, J.P. Chittoor, S. Krishnapillai, *Mini Rev. Org. Chem.* **1**, 375 (2004)
44. M. Umkehrer, J. Kolb, C. Burdack, W. Hiller, *Synlett* **2005**, 79 (2005)
45. T.D. Gordon, J. Singh, P.E. Hansen, B.A. Morgan, *Tetrahedron Lett.* **34**, 1901 (1993)
46. N. Desroy, F. Moreau, S. Briet, G. Le Fralliec, S. Floquet, L. Durant, V. Vongsouthi, V. Gerusz, A. Denis, S. Escaich, *Biorg. Med. Chem.* **17**, 1276 (2009)
47. E. Bey, S. Marchais-Oberwinkler, R. Werth, M. Negri, Y.A. Al-Soud, P. Kruchten, A. Oster, M. Frotscher, B. Birk, R.W. Hartmann, *J. Med. Chem.* **51**, 6725 (2008)
48. R. Breslow, *J. Am. Chem. Soc.* **80**, 3719 (1958)
49. S. Tani, T.N. Uehara, J. Yamaguchi, K. Itami, *Chem. Sci.* **5**, 123 (2014)
50. A. Cohen, M.D. Crozet, P. Rathelot, P. Vanelle, *Green Chem.* **11**, 1736 (2009)
51. G.L. Turner, J.A. Morris, M.F. Greaney, *Angew. Chem.* **119**, 8142 (2007)
52. K.J. Hodgetts, M.T. Kershaw, *Org. Lett.* **5**, 2911 (2003)
53. T.S. Jagodzinski, *Chem. Rev.* **103**, 197 (2003)
54. S.L. You, J.W. Kelly, *J. Org. Chem.* **68**, 9506 (2003)
55. S. Bondock, W. Khalifa, A.A. Fadda, *Eur. J. Med. Chem.* **42**, 948 (2007)
56. K.M. Weiß, S. Wei, S.B. Tsogoeva, *Org. Biomol. Chem.* **9**, 3457 (2011)
57. S. Murru, A. Nefzi, *ACS Comb. Sci.* **16**, 39 (2014)
58. J.V. Metzger, in *Comprehensive Heterocyclic Chemistry*, vol. 6, ed. by A.R. Katritzky, C.W. Rees (Pergamon, New York, 1984), p. 235
59. A. Dondoni, P. Merino, in *Comprehensive Heterocyclic Chemistry II*, vol. 3, ed. by A.R. Katritzky, C.W. Rees, E.F.V. Scriven (Elsevier, New York, 1996), p. 373
60. A. Hantzsch, J.H. Weber, *Eur. J. Inorg. Chem.* **20**, 3118 (1887)
61. T. Bach, S. Heuser, *Tetrahedron Lett.* **41**, 1707 (2000)
62. J.S. Carter, D.J. Rogier, M.J. Graneto, K. Seibert, C.M. Koboldt, Y. Zhang, J.J. Talley, *Biorg. Med. Chem. Lett.* **9**, 1167 (1999)
63. G.M. Atkins, E.M. Burgess, *J. Am. Chem. Soc.* **90**, 4744 (1968)
64. S. Vijay Kumar, G. Parameshwarappa, H. Ila, *J. Org. Chem.* **78**, 7362 (2013)
65. A. Dondini, *Org. Biomol. Chem.* **8**, 3366 (2010)
66. J. Kolb, B. Beck, A. Domling, *Tetrahedron Lett.* **43**, 6897 (2002)
67. H. Zheng, Y.J. Mei, K. Du, X.T. Cao, P.F. Zhang, *Molecules* **18**, 13425 (2013)
68. S.Z. SayyedAlangi, Z. Hossaini, F. Rostami-Charati, H. SajjadiGhotabadi, *Comb. Chem. High Throughput Screen.* **16**, 758 (2013)
69. S. Karamthulla, S. Pal, M.N. Khan, L.H. Choudhury, *RSC Adv.* **4**, 37889 (2014)
70. N. Razavi, B. Akhlaghinia, *RSC Adv.* **5**, 12372 (2015)
71. R. Jahanshahi, B. Akhlaghinia, *Catal. Lett.* **147**, 2640 (2017)
72. R. Jahanshahi, B. Akhlaghinia, *RSC Adv.* **5**, 104087 (2015)
73. R. Jahanshahi, B. Akhlaghinia, *RSC Adv.* **6**, 29210 (2016)
74. M. Nejatianfar, B. Akhlaghinia, R. Jahanshahi, *Appl. Organomet. Chem.* (2017)
75. S.S.E. Ghodsinia, B. Akhlaghinia, R. Jahanshahi, *RSC Adv.* **6**, 63613 (2016)
76. N. Razavi, B. Akhlaghinia, R. Jahanshahi, *Catal. Lett.* **147**, 360 (2017)
77. R. Jahanshahi, B. Akhlaghinia, *Chem. Pap.* **71**, 1351 (2017)
78. M. Esmailpour, B. Akhlaghinia, R. Jahanshahi, *J. Chem. Sci.* **129**, 313 (2017)
79. R. Jahanshahi, B. Akhlaghinia, *New J. Chem.* **41**, 7203 (2017)
80. M. Zarghani, B. Akhlaghinia, *RSC Adv.* **5**, 87769 (2015)
81. Z. Zarei, B. Akhlaghinia, *RSC Adv.* **6**, 106473 (2016)
82. M.S. Ghasemzadeh, B. Akhlaghinia, *Bull. Chem. Soc. Jpn.* **90**, 1119 (2017)
83. N. Mohammadian, B. Akhlaghinia, *Res. Chem. Intermed.* **43**, 3225 (2017)
84. A. Mohammadinezhad, B. Akhlaghinia, *Aust. J. Chem.* (2017)
85. A. Mohammadinezhad, B. Akhlaghinia, *Green Chem.* **19**, 5625 (2017)
86. Z. Zarei and B. Akhlaghinia, *New J. Chem.* (2017)
87. D. Zhao, Q. Huo, J. Feng, B.F. Chmelka, G.D. Stucky, *J. Am. Chem. Soc.* **120**, 6024 (1998)
88. E. Kolvari, N. Koukabi, M.M. Hosseini, *J. Mol. Catal. A Chem.* **397**, 68 (2015)

89. M. Aghayee, M.A. Zolfigol, H. Keypour, M. Yarie, L. Mohammadi, *Appl. Organomet. Chem.* **30**, 612 (2016)
90. F. Adam, K.M. Hello, H. Osman, *Chin. J. Chem.* **28**, 2383 (2010)
91. Z.H. Zhang, K. Dong, Z.B. Zhao, *Chemsuschem* **4**, 112 (2011)
92. F. Su, Q. Wu, D. Song, X. Zhang, M. Wang, Y. Guo, *J. Mater. Chem.* **1**, 13209 (2013)
93. C.W. Young, P.C. Servais, C.C. Currie, M.J. Hunter, *J. Am. Chem. Soc.* **70**, 3758 (1948)
94. Z. Gao, L. Wang, T. Qi, J. Chu, Y. Zhang, *Colloids Surf. A* **304**, 77 (2007)
95. B. Karimi, M. Khorasani, *ACS Catal.* **3**, 1657 (2013)
96. B. Karimi, M. Vafaezadeh, *RSC Adv.* **3**, 23207 (2013)
97. B. Karimi, H. Mirzaei, *RSC Adv.* **3**, 20655 (2013)
98. S. Rostamnia, H. Xin, *Appl. Organomet. Chem.* **27**, 348 (2013)
99. S. Rostamnia, H. Xin, X. Liuand, K. Lamei, *J. Mol. Catal. A Chem.* **85**, 374 (2013)
100. S. Rostamnia, F. Pourhassan, *Chin. Chem. Lett.* **24**, 401 (2013)
101. W. Xie, M. Fan, *Chem. Eng. J.* **239**, 60 (2014)
102. P. Sharma, A.P. Singh, *Catal. Sci. Technol.* **4**, 2978 (2014)